Inhibition of SARS-CoV-2 main protease 3CL^pro by means of α-ketoamide and pyridone-containing pharmaceuticals using in silico molecular docking

Amin O. Elzupir

Imam Mohammad Ibn Saud Islamic University (IMSIU), College of Science, Deanship of Scientific Research, Riyadh, KSA

A B S T R A C T

The coronavirus disease infections (COVID-19) caused by a new type of coronavirus (SARS-CoV-2) have been emerging in the entire world. Therefore, it is necessary to find out potential therapeutic pharmaceuticals for this disease. This study investigates the inhibitory effect of the 3-chymotrypsin-like protease of SARS-CoV-2 (3CL^pro) using pharmaceuticals containing α-ketoamide group and pyridone ring based on molecular docking. Of these, eight pharmaceuticals approved by US-Food and Drug Administration have shown good contact with the catalytic residues of 3CL^pro. They are telaprevir, temsirolimus, pimecrolimus, aminoglutethimide, apixaban, buspirone, lenalidomide, and pomalidomide. Their binding affinity score ranged from -5.6 to -7.4 kcal/mol. Hydrogen bonds were observed and reported. To the knowledge, this study report for the first time a compound that could be binding to ALA^285, the new residue resulting from genetic modification of 3CL^pro of SARS-CoV-2 that has increased its catalytic activity 3.6-fold compared with its predecessor 3CL^pro of SARS-CoV. It is recommended that telaprevir, and pyridone-containing pharmaceuticals including aminoglutethimide, apixaban, buspirone, lenalidomide, and pomalidomide be repurposed for COVID-19 treatment after suitable validation and clinical trials.

© 2020 Elsevier B.V. All rights reserved.

1. Introduction

In December 2019, a novel coronavirus named SARS-CoV-2 was reported, after an outbreak-pandemic of the pulmonary disease in Wuhan city in China called coronavirus disease-19 (COVID-19). The causes of the first infections were attributed to foods made from bat and bat-like animals. Then COVID-19 were melodramatically spread by human-to-human transmission through all the world. As of April 25, 2000, confirmed cases worldwide were 2,803,571, and mortality was 195,997 according to the Asian news network [1–4]. The most important symptoms of COVID-19 are high fever, dyspnea, nonproductive cough, headache, fatigue, difficulty breathing, and frost-glass-like symptoms in the lungs [5–7].

Coronaviruses have the largest RNA genomes (27 to 31 KB) compared to other viruses. SARS-CoV-2 are positive-stranded RNA viruses and belongs to class b of the genus *Betacoronavirus.* recent studies have shown that the RNA genomes of SARS-CoV-2 are identical to about 82% of that of SARS-CoV [8–11]. The 229E gene encodes two polyproteins involved in releasing of functional polypep-

tides, that are essential for viral replication and transcription. The extensive proteolytic processing responsible from the production of the polypeptides is achieved by the 3-chymotrypsin-like protease of SARS-CoV-2 (M^pro, or 3CL^pro), as it cleaves at least 11 sites on the polyproteins translated from the viral RNA. Thus, drugs that inhibit this enzyme can be an effective therapeutic agent for COVID-19 [12,13].

Recently several studies have been conducted on some pharmaceuticals, synthetic and natural products to study their ability to inhibit 3CL^pro using the molecular docking approach. Of these tested drugs are darunavir, favipiravir isoflavone, myricitrin, chloroquine phosphate, remdesivir, indinavir, valrubicin, lopinavir, carfilzomib, eravacycline, elbasvir, and methyl rosmarinate [14–20]. Zhang el. have reported α-ketoamide and pyridone containing-synthetic compounds with a good inhibitory effect against 3CL^pro [21]. However, more research is still needed in this regard, the aim of this research study was to investigate the inhibitory effect of 3CL^pro using approved drugs that contain α-ketoamide group and pyridone ring.
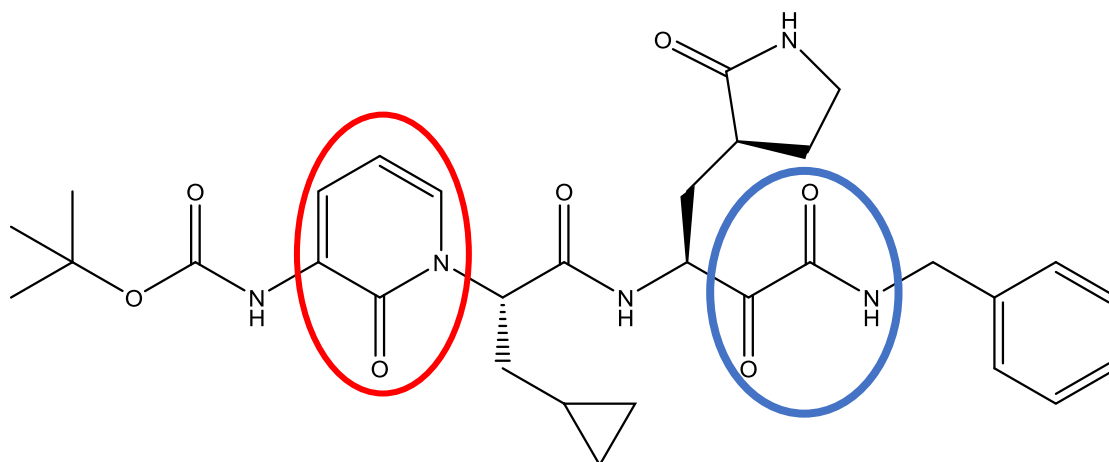
Scheme 1. Chemical structure of reference compound.

2. Materials and methods

2.1. Pharmaceuticals containing α-ketoamide group and pyridone ring

The DrugBank database search engine has used to find α-ketoamide and pyridone-containing drugs. Based on these criteria, twelve drugs approved by the U.S. Food and Drug Administration were found. Six of them have α-ketoamide functional group are telaprevir, temsirolimus, pimecrolimus, everolimus, sirolimus, and tacrolimus. While pyridone-containing-pharmaceuticals are aminoglutethimide, apixaban, buspirone, lenalidomide, pomalidomide, and ubrogepant.

2.2. Buildup and energy minimization of the molecular structures

The three-dimensional structures generated and minimized via UCSF Chimera software (v 1.10.2.), using the smile string code offered by the PubChem database. The crystal structure of 3-chymotrypsin-like protease (3CL^{pro}) of SARS-CoV-2 was obtained from the Protein Data Bank database (PDB ID: 6Y2E).

2.3. Molecular docking

Molecular docking experiments performed utilizing AutoDock Vina tool implemented in UCSF Chimera software v 1.10.2., adopting the default values for the parameters, and a grid box (-16.302 × -26.086 × 17.551) Å centered at (29.176, 58.386, 75.078) Å. Water was added as a solvent with a total solvent accessible surface area of 14358.5. The predicted score values (binding affinity) were explored using View Dock tool. The verify of docking results, binding sites, and image processing were conducted using UCSF Chimera [22–24].

3. Results and discussion

The α-ketoamide and pyridone-containing synthetic compound used as a reference in this study docked with 3CL^{pro} containing water residues as a solvent to represents the real environment. It was showed a good inhibitory effect with binding affinity ranged between -5.0 to -6.0 kcal/mole. The chemical structure of the reference compound was monitored in Scheme 1, α-ketoamide functional group and pyridone ring were indicated by blue and red circles, respectively [21]. The search on the DrugBank database revealed that there is no pharmaceutical containing both of the functional groups. Of the α-ketoamide set, everolimus, eirolimus, and tacrolimus have excluded because those drugs were approved as immunosuppressive agents. Whereas, ubrogepant belongs to pyridone containing-drugs was showed no binding affinity to the active residues of CL^{pro}. The binding affinity score of the remaining pharmaceuticals with CL^{pro} were ranged from -5.6 to -7.4 kcal/mol (Tables 1 and 2).

The inhibitory effect of CL^{pro} was investigated based on hydrogen-bonds and Van der Waals interactions between the selected drugs and the catalytic residues of CL^{pro} (Cys^{145} and His^{41}), the important residues for keeping the enzyme on the correct conformation (Ser^1 and Glu^{166}), and the residue resulting from the genetic mutation that led to a 3.6-fold increase in the reproductive effectiveness of the virus (Ala^{285}) [3,21]. Telaprevir, the anti-hepatitis B virus has the most potent activity among the α-ketoamide-containing drugs. Maybe its activity could be increased by combination use with temsirolimus that used for the treatment of renal cell carcinoma. Figs. 1-3 show the interactions between these drugs and CL^{pro}, Hydrogen bonds in blue stripes, and Van der Waals yellow stripes.

The pyridone-containing pharmaceuticals have shown a tendency to interacts with His^{41} and other active residues as shown in Figs. 4-8. Of these, aminoglutethimide is used in the treatment of seizures, breast cancer, and prostate cancer [25,26]. Aminoglutethimide has shown the latest binding affinity, however, is interacts with Cys^{145} also and has an ability to make hydrogen bonds with Glu^{166}. Buspirone, lenalidomide, and pomalidomide are approved in 1986, 2005, and 2013, respectively. They are used to treat anxiety disorders, multiple myeloma, and anemia [27–29]. These three medications may be the best inhibitors for CL^{pro} as they have shown a significant tendency to make hydrogen bonds with Cys^{145}, however, apixaban may be an exception. Apixaban is approved in 2012 for the prevention and treatment of thromboembolic diseases, its advantage has an ability to bind with the Ala^{285}. In this group, the pyridone ring played a key role in inhibiting the CL^{pro}, by making hydrogen bonds with the catalytic residues. The thing that opens the door is wide for many researches into developing new simple inhibitors of this enzyme, as in fact, the pyridone-containing pharmaceuticals are very simple and easy to produce in large commercial quantities commensurate with the spread of this pandemic.

To sum, telaprevir, aminoglutethimide, apixaban, buspirone, lenalidomide, and pomalidomide have shown a good binding affinity to the catalytic sites of CL^{pro}. This study suggests the repurposing of these drugs for COVID-19 treatment after a suitable *in vitro* and *in vivo* validation as well as clinical trials. To the knowledge, this study report for the first time a 3CL^{pro} inhibitor regarding their contacts with ALA^{285}.

Table 1
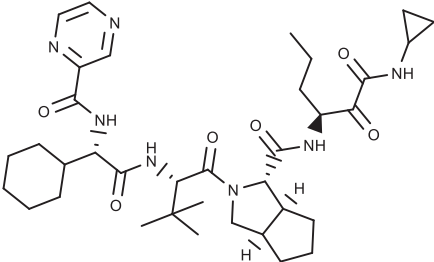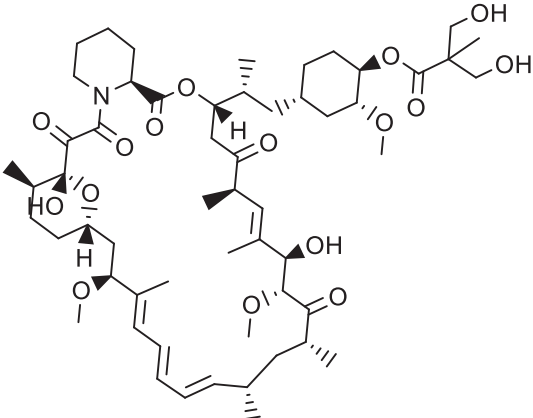The binding affinity of the α-ketoamide-containing pharmaceuticals with 3-chymotrypsin-like protease (CLpro).
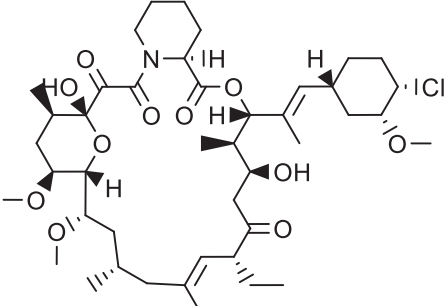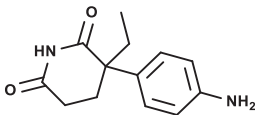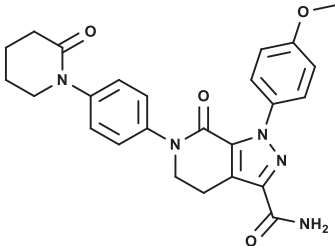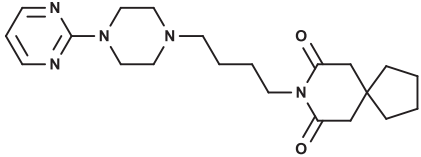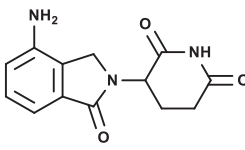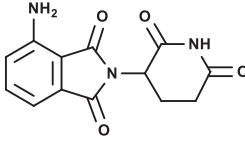
Pharmaceutical name	Structure	Score (kcal/mol)	RMSD	Hydrogen bond	Van der Waals (distance)
Telaprevir		-5.9	25.88 - 30.63	Glu[166]	His[41] (3.185 Å/ 3.334 Å/ 3.574 Å/ 3.796 Å). Cys[145] (3.553Å/ 3.826 Å). Glu[166] (17 side contacts, distance range: 3.201Å to 3.920 Å)
Temsirolimus		-7.1	2.41 - 7.91	-	Ala[285] (3.436 Å)
Pimecrolimus		-6.7	31.63 - 34.72	-	Glu[166] (13 side contacts, distance range: 2.817Å to 4.113 Å)

Table 2
The binding affinity of the pyridone-containing pharmaceuticals with 3-chymotrypsin-like protease (CLpro).

| Pharmaceutical name	Structure	Score (kcal/mol)	RMSD	Hydrogen bond (distance)	Van der Waals (distance)
Aminoglutethimide		-5.6	1.85 - 2.35	Glu[166] (2.480Å/ 2.647Å)	Cys[145] (4.027Å). His[41] (distance: 3.331Å/ 3.599 Å/ 3.889Å). Glu[166] (14 side contacts, distance range: 2.480Å to 4.034Å).
Apixaban		-7.4	23.15 - 25.97	-	Ala[285] (3.302Å/ 3.546 Å). His[41] (distance: 2.720 Å/ 2.875 Å/ 2.948 Å/ 3.131Å/ 3.635Å). Glu[166] (6 side contacts, distance range: 3.423Å to 4.076Å)
Buspirone		-6.9	2.02 -7.79	Cys[145] Glu[166]	His[41] (3.531 Å/ 3.708 Å/ 3.762 Å/ 3.951 Å). Cys[145] (distance: 3.831Å). Glu[166] (12 side contacts, distance range: 3.107 Å to 4.142 Å).
Lenalidomide		-6.5	27.28 - 29.07	Cys[145] Glu[166]	His[41] (distance: 3.324 Å). Cys[145] (distance: 3.814 Å). Glu[166] (9 side contacts, distance range: 3.137 Å to 3.919 Å).
Pomalidomide		-6.6	1.69 -3.04	Cys[145] Glu[166]	His[41] (distance: 3.377 Å). Cys[145] (distance: 3.616 Å/ 3.823 Å). Glu[166] (13 side contacts, distance range: 2.310 Å to 3.948 Å).
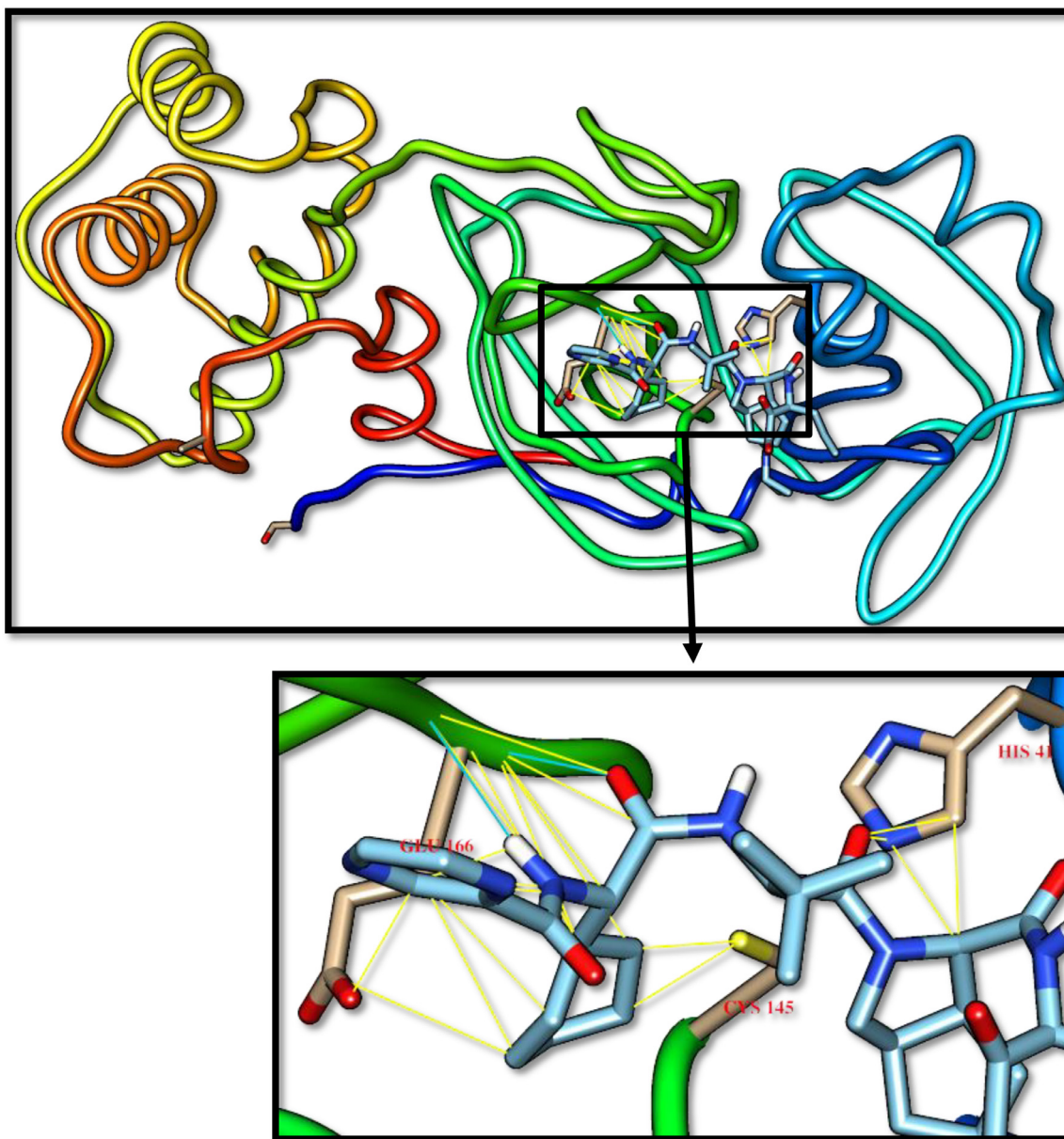
Fig. 1. Telaprevir docked with 3-chymotrypsin-like protease (3CL^{pro}) of SARS-CoV-2. Hydrocarbon skeleton of telapreviris cyan, nitrogen atoms are blue, oxygens red. Below, a magnified images of contact sites of telapreviris with HIS^{41}, CYS^{145} and GLU^{166}. (For interpretation of the references to color in this figure legend, the reader is referred to the web version of this article.)
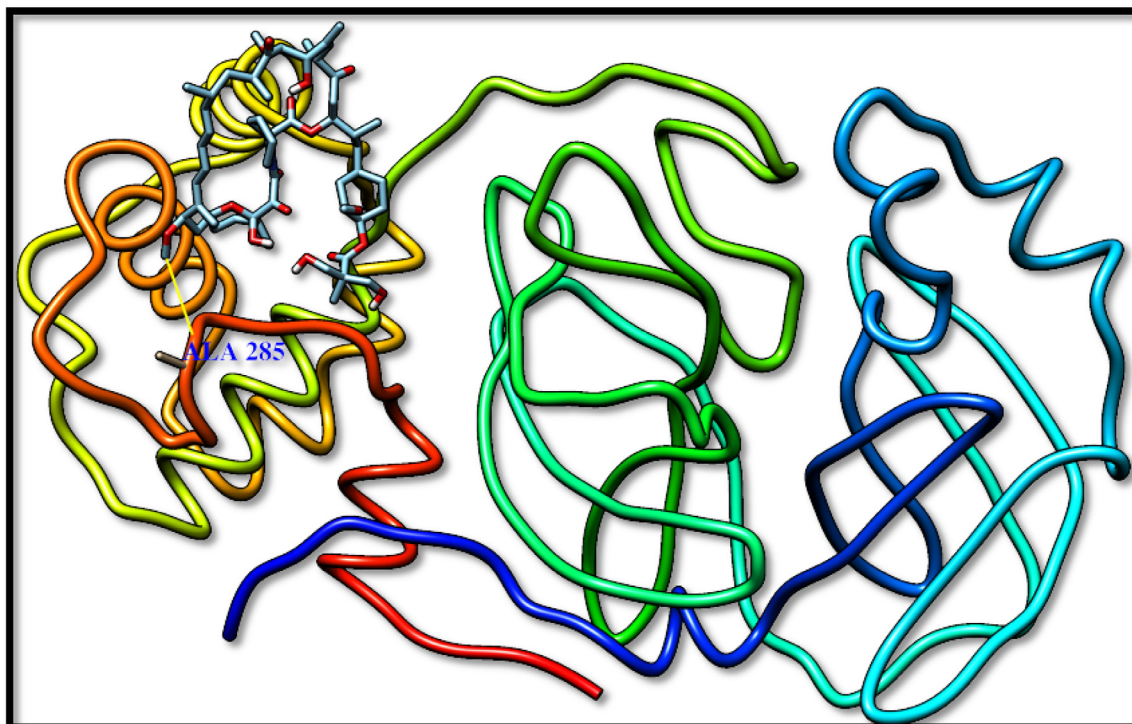
Fig. 2. Temsirolimus docked with 3-chymotrypsin-like protease (3CL^pro) of SARS-CoV-2. Hydrocarbon skeleton of temsirolimuscyan, nitrogen atoms are blue, oxygens red. (For interpretation of the references to color in this figure legend, the reader is referred to the web version of this article.)
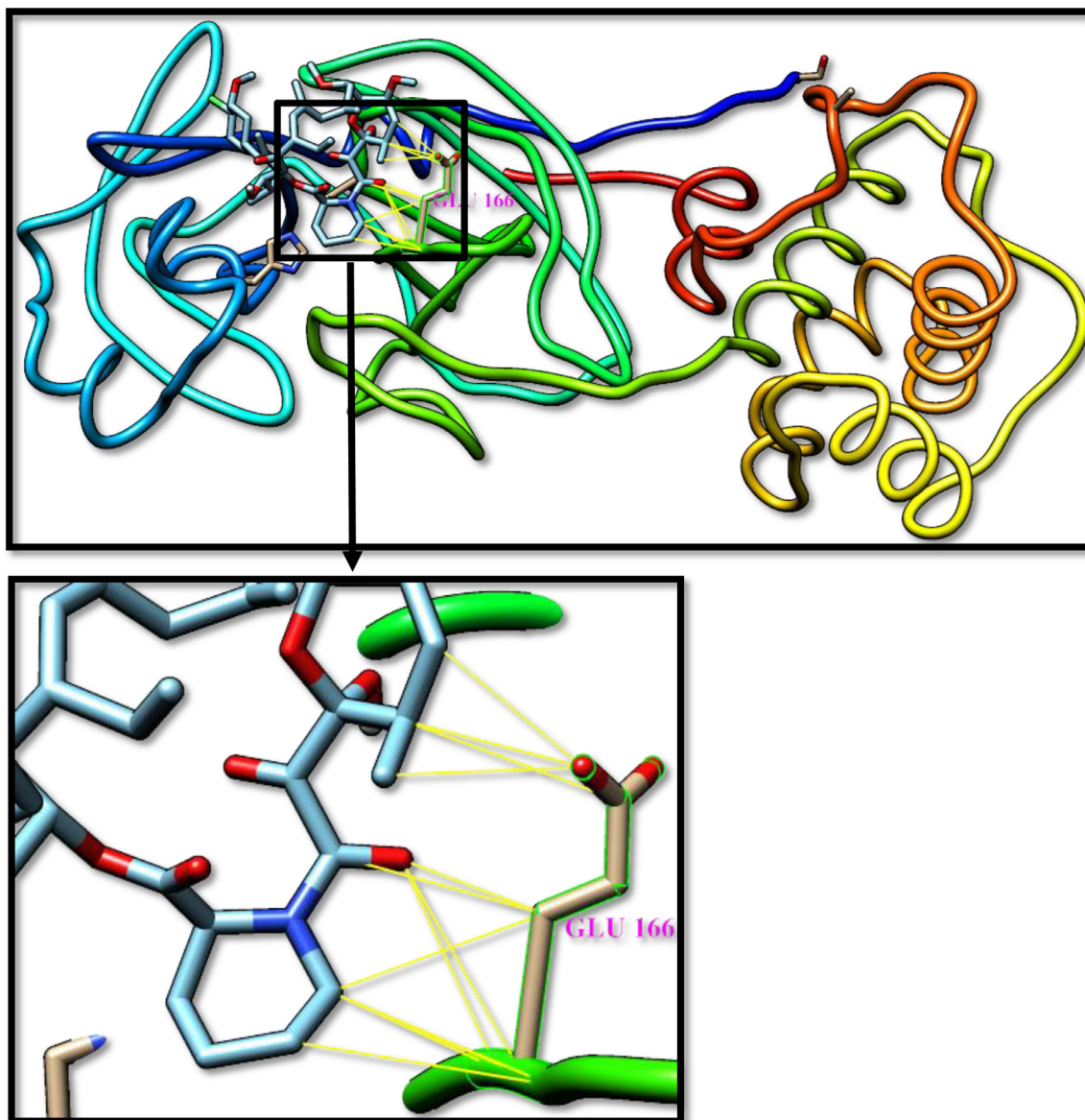
Fig. 3. Pimecrolimus docked with 3-chymotrypsin-like protease (3CL^{pro}) of SARS-CoV-2. Hydrocarbon skeleton of pimecrolimus, nitrogen atoms are blue, oxygens red. Below, a magnified images of contact sites of pimecrolimus with GLU^{166}. (For interpretation of the references to color in this figure legend, the reader is referred to the web version of this article.)

Fig. 4. Aminoglutethimide docked with 3-chymotrypsin-like protease (3CL^{pro}) of SARS-CoV-2. Hydrocarbon skeleton of Aminoglutethimide is cyan, nitrogen atoms are blue, oxygens red. Below, a magnified images of contact sites of Aminoglutethimide with HIS[41], CYS[145] and GLU[166]. (For interpretation of the references to color in this figure legend, the reader is referred to the web version of this article.)

Fig. 5. Apixaban docked with 3-chymotrypsin-like protease (3CL^{pro}) of SARS-CoV-2. Hydrocarbon skeleton of apixaban is cyan, nitrogen atoms are blue, oxygens red. Below, different side of view of magnified images of contact sites of apixaban with ALA^{285}, HIS^{41}, and GLU^{166}. (For interpretation of the references to color in this figure legend, the reader is referred to the web version of this article.)

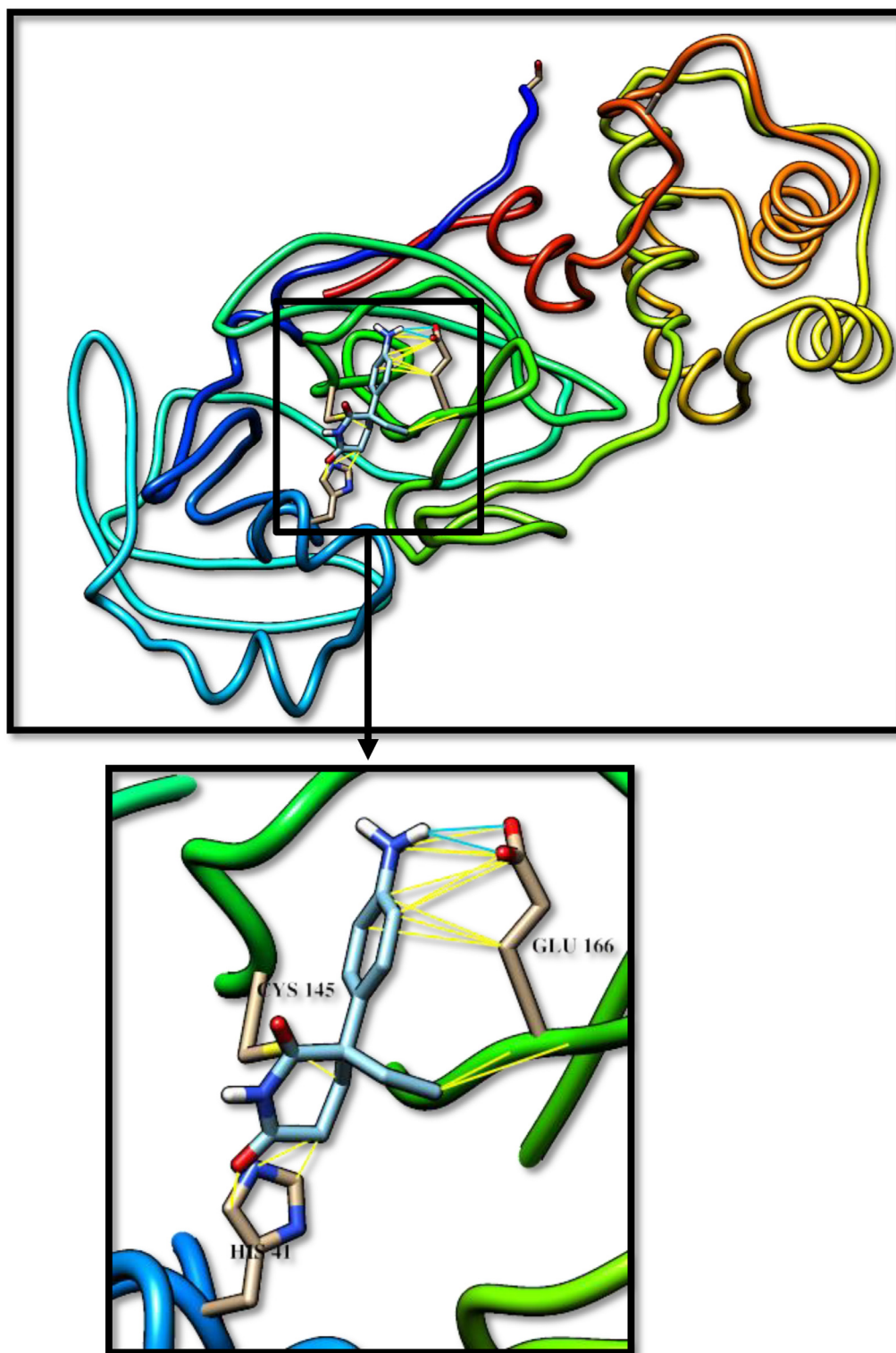**Fig. 6.** Buspirone docked with 3-chymotrypsin-like protease (3CL^{pro}) of SARS-CoV-2. Hydrocarbon skeleton of buspirone is cyan, nitrogen atoms are blue, oxygens red. Below, different side of view of a magnified images of contact sites of Buspirone with HIS^{41}, CYS^{145} and GLU^{166}. (For interpretation of the references to color in this figure legend, the reader is referred to the web version of this article.)
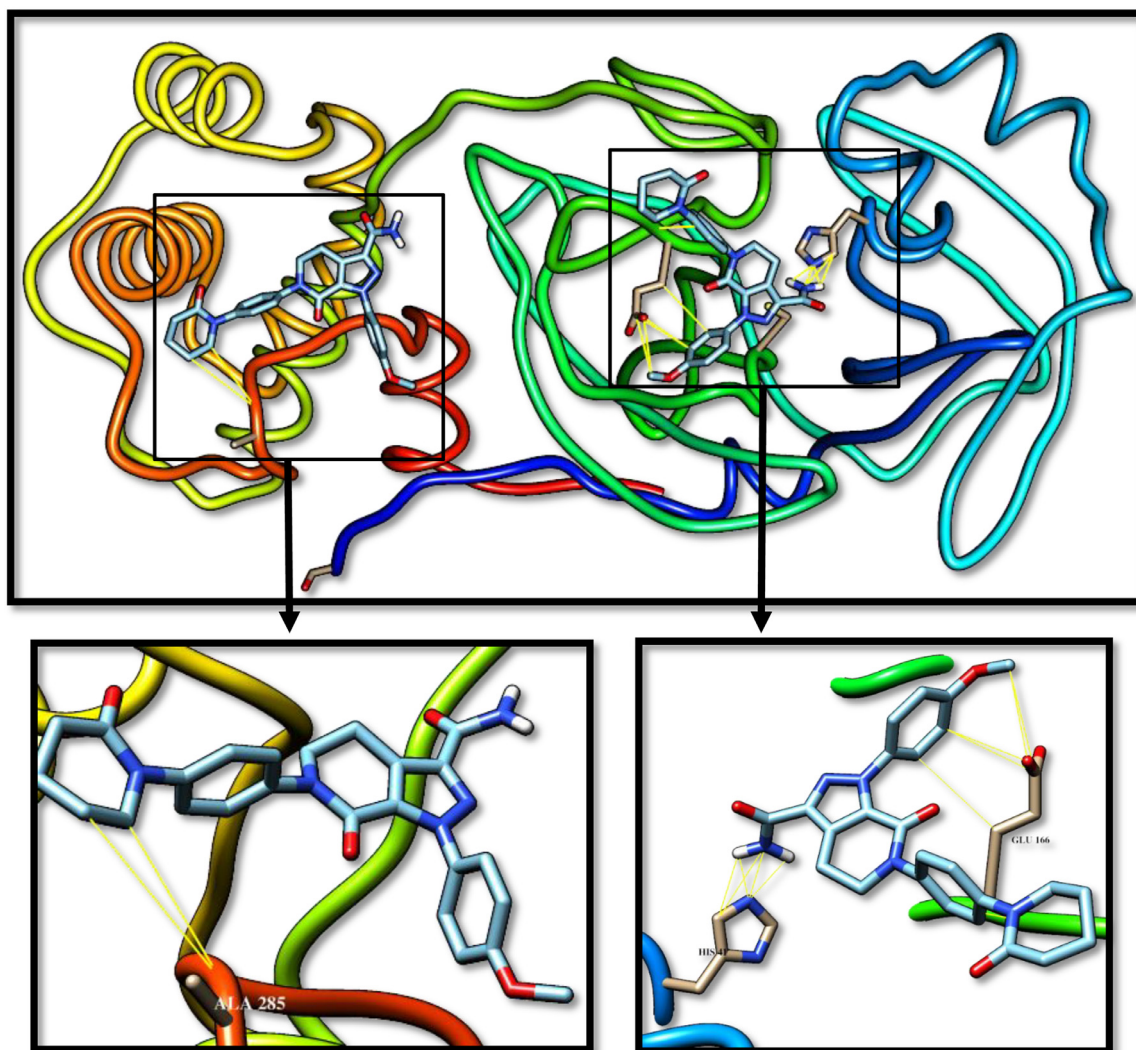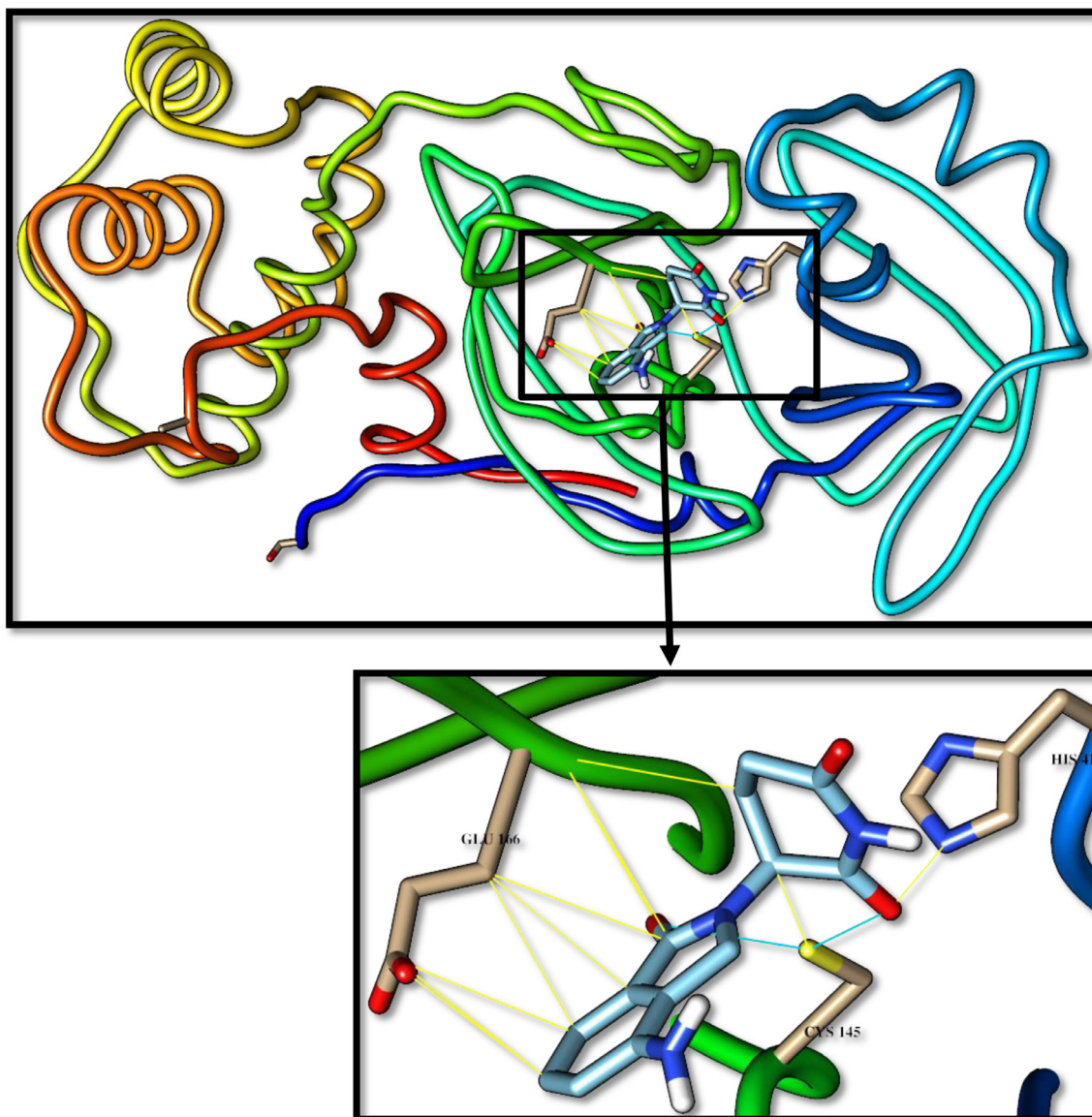
Fig. 7. Lenalidomide docked with 3-chymotrypsin-like protease (3CL^{pro}) of SARS-CoV-2. Hydrocarbon skeleton of lenalidomide is cyan, nitrogen atoms are blue, oxygens red. Below, different side of view of a magnified images of contact sites of lenalidomide with HIS^{41}, CYS^{145} and GLU^{166}. (For interpretation of the references to color in this figure legend, the reader is referred to the web version of this article.)
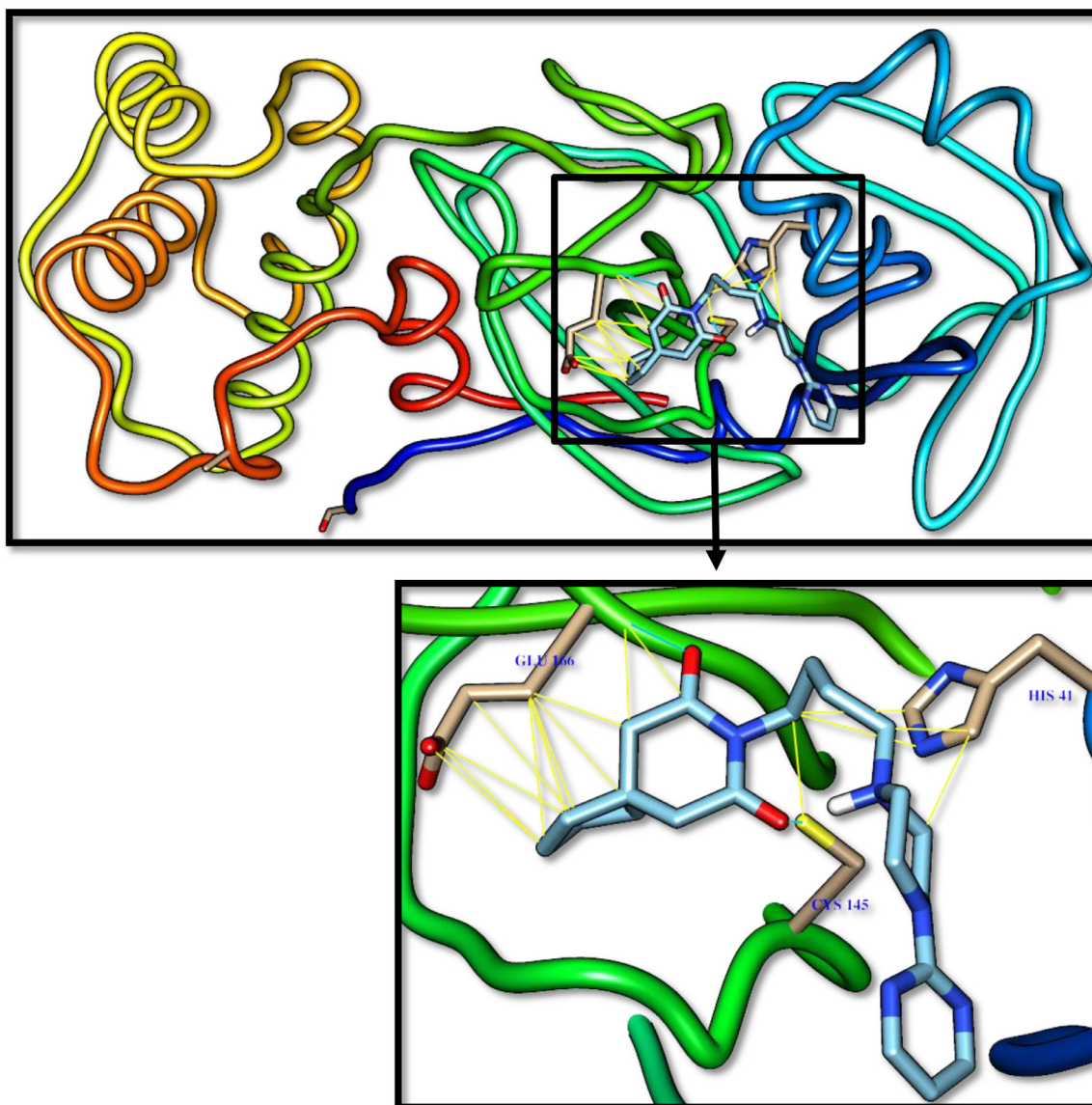
Fig. 8. Pomalidomide docked with 3-chymotrypsin-like protease (3CL^pro) of SARS-CoV-2. Hydrocarbon skeleton of pomalidomide is cyan, nitrogen atoms are blue, oxygens red. Below, different side of view of a magnified images of contact sites of pomalidomide with HIS[41], CYS[145] and GLU[166]. (For interpretation of the references to color in this figure legend, the reader is referred to the web version of this article.)
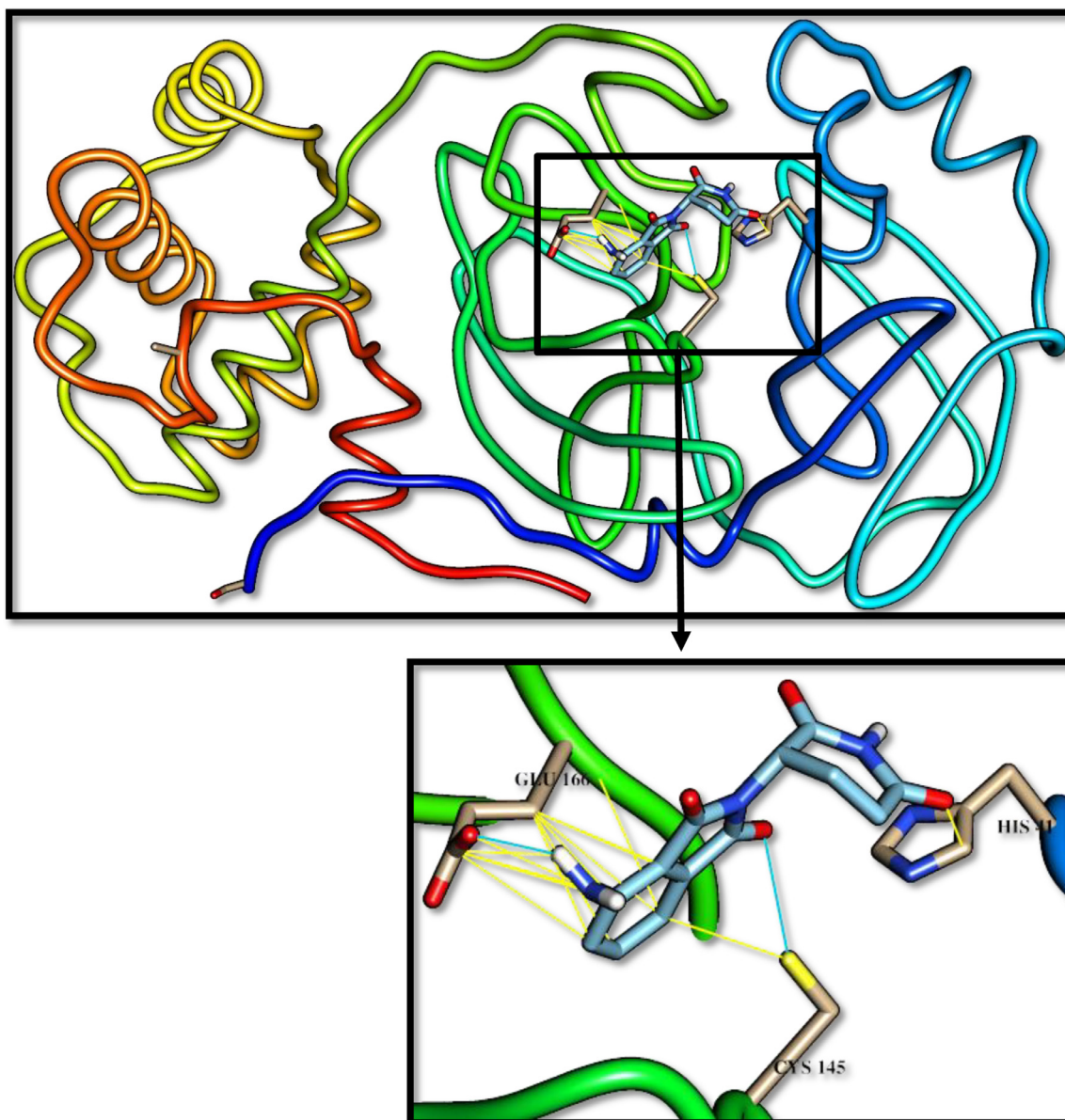
Data availability

The data will be available upon request.

Declaration of Competing Interest

The author declares that he has no conflict of interest.

CRediT authorship contribution statement

Amin O. Elzupir: Conceptualization, Investigation, Methodology, Software, Writing - review & editing.

References

[1] H.A. Rothan, S.N. Byrareddy, The epidemiology and pathogenesis of coronavirus disease (COVID-19) outbreak, J. Autoimmun. (2020) 102433.

[2] T.P. Velavan, C.G. Meyer, The COVID-19 epidemic, Trop. Med. Int. Health 25 (3) (2020) 278–280.

[3] J. Chen, T. Qi, L. Liu, Y. Ling, Z. Qian, T. Li, F. Li, Q. Xu, Y. Zhang, S. Xu, Clinical progression of patients with COVID-19 in Shanghai, China, J. Infect. (2020).

[4] D. Chang, M. Lin, L. Wei, L. Xie, G. Zhu, C.S.D. Cruz, L. Sharma, Epidemiologic and clinical characteristics of novel coronavirus infections involving 13 patients outside Wuhan, China, JAMA (2020).

[5] W. Liu, H. Li, COVID-19 disease: ORF8 and surface glycoprotein inhibit heme metabolism by binding to porphyrin, ChemRxiv (2020).

[6] K. Diao, P. Han, T. Pang, Y. Li, Z. Yang, HRCT imaging features in representative imported cases of 2019 novel coronavirus pneumonia, Precis. Clin. Med. 3 (1) (2020) 9–13.

[7] C. Huang, Y. Wang, X. Li, L. Ren, J. Zhao, Y. Hu, L. Zhang, G. Fan, J. Xu, X. Gu, Clinical features of patients infected with 2019 novel coronavirus in Wuhan, China, Lancet North Am. Ed. 395 (10223) (2020) 497–506.

[8] N. Zhu, D. Zhang, W. Wang, X. Li, B. Yang, J. Song, X. Zhao, B. Huang, W. Shi, R. Lu, China Novel Coronavirus Investigating and Research Team. A novel coronavirus from patients with pneumonia in China, 2019, N. Engl. J. Med. 382 (8) (2020) 727–733.

[9] P. Zhou, X.-L. Yang, X.-G. Wang, B. Hu, L. Zhang, W. Zhang, H.-R. Si, Y. Zhu, B. Li, C.-L. Huang, A pneumonia outbreak associated with a new coronavirus of probable bat origin, Nature 579 (7798) (2020) 270–273.

[10] F. Wu, S. Zhao, B. Yu, Y.-M. Chen, W. Wang, Z.-G. Song, Y. Hu, Z.-W. Tao, J.-H. Tian, Y.-Y. Pei, A new coronavirus associated with human respiratory disease in China, Nature 579 (7798) (2020) 265–269.

[11] R. Lu, X. Zhao, J. Li, P. Niu, B. Yang, H. Wu, W. Wang, H. Song, B. Huang, N. Zhu, Genomic characterisation and epidemiology of 2019 novel coronavirus: implications for virus origins and receptor binding, Lancet North Am. Ed. 395 (10224) (2020) 565–574.

[12] K. Anand, J. Ziebuhr, P. Wadhwani, J.R. Mesters, R. Hilgenfeld, Coronavirus main proteinase (3CLpro) structure: basis for design of anti-SARS drugs, Science 300 (5626) (2003) 1763–1767.

[13] M.A. Shereen, S. Khan, A. Kazmi, N. Bashir, R. Siddique, COVID-19 infection: origin, transmission, and characteristics of human coronaviruses, J. Adv. Res. (2020).

[14] A.A. Elfiky, Anti-HCV, nucleotide inhibitors, repurposing against COVID-19, Life Sci. (2020) 117477.

[15] Y. Duan, H.-L. Zhu, C. Zhou, Advance of promising targets and agents against 2019-nCoV in China, Drug Discov. Today (2020).

[16] B.R. Beck, B. Shin, Y. Choi, S. Park, K. Kang, Predicting commercially available antiviral drugs that may act on the novel coronavirus (SARS-CoV-2) through a drug-target interaction deep learning model, Comput. Struct. Biotechnol. J. (2020).

[17] M.T. ul Qamar, S.M. Alqahtani, M.A. Alamri, L.-L. Chen, Structural basis of SARS-CoV-2 3CLpro and anti-COVID-19 drug discovery from medicinal plants, J. Pharm. Anal. (2020).

[18] C. Wu, Y. Liu, Y. Yang, P. Zhang, W. Zhong, Y. Wang, Q. Wang, Y. Xu, M. Li, X. Li, Analysis of therapeutic targets for SARS-CoV-2 and discovery of potential drugs by computational methods, Acta Pharm. Sin. B (2020).

[19] J. Wang, Fast identification of possible drug treatment of coronavirus disease-19 (COVID-19) through computational drug repurposing study, (2020).

[20] Y.-C. Chang, Y.-A. Tung, K.-H. Lee, T.-F. Chen, Y.-C. Hsiao, H.-C. Chang, T.-T. Hsieh, C.-H. Su, S.-S. Wang, J.-Y. Yu, Potential therapeutic agents for COVID-19 based on the analysis of protease and RNA polymerase docking, (2020).

[21] L. Zhang, D. Lin, X. Sun, U. Curth, C. Drosten, L. Sauerhering, S. Becker, K. Rox, R. Hilgenfeld, Crystal structure of SARS-CoV-2 main protease provides a basis for design of improved α-ketoamide inhibitors, Science (2020).

[22] O. Trott, A.J. Olson, AutoDock Vina: improving the speed and accuracy of docking with a new scoring function, efficient optimization, and multithreading, J. Comput. Chem. 31 (2) (2010) 455–461.

[23] E.F. Pettersen, T.D. Goddard, C.C. Huang, G.S. Couch, D.M. Greenblatt, E.C. Meng, T.E. Ferrin, UCSF Chimera—a visualization system for exploratory research and analysis, J. Comput. Chem. 25 (13) (2004) 1605–1612.

[24] R.C. Edgar, B.J. Haas, J.C. Clemente, C. Quince, R. Knight, UCHIME improves sensitivity and speed of chimera detection, Bioinformatics 27 (16) (2011) 2194–2200.

[25] R.J. Santen, R.I. Misbin, Aminoglutethimide: review of pharmacology and clinical use, Pharmacotherapy 1 (2) (1981) 95–119.

[26] S.B. Kaye, R.L. Woods, R.M. Fox, A.S. Coates, M.H. Tattersall, Use of aminoglutethimide as second-line endocrine therapy in metastatic breast cancer, Cancer Res. 42 (8 Supplement) (1982) 3445s–3447s.

[27] J.S. New, The discovery and development of buspirone: a new approach to the treatment of anxiety, Med. Res. Rev. 10 (3) (1990) 283–326.

[28] A. List, S. Kurtin, D.J. Roe, A. Buresh, D. Mahadevan, D. Fuchs, L. Rimsza, R. Heaton, R. Knight, J.B. Zeldis, Efficacy of lenalidomide in myelodysplastic syndromes, N. Engl. J. Med. 352 (6) (2005) 549–557.

[29] A. Chanan-Khan, A. Swaika, A. Paulus, S.K. Kumar, J.R. Mikhael, S.V. Rajkumar, A. Dispenzieri, M. Lacy, Pomalidomide: the new immunomodulatory agent for the treatment of multiple myeloma, Blood Cancer J. 3 (9) (2013) e143 e143.